



Enhanced electropromotion of methane combustion on palladium catalysts deposited on highly porous supports

F. Matei^a, C. Jiménez-Borja^b, J. Canales-Vázquez^c, S. Brosda^{d,*}, F. Dorado^b, J.L. Valverde^b, D. Ciuparu^{a,**}

^a Department of Petroleum Processing Engineering and Environmental Protection, Petroleum – Gas University of Ploiești, 39 București Bd, 100680 Ploiești, Romania

^b Department of Chemical Engineering, Universidad de Castilla-La Mancha (UCLM), Avda. Camilo José Cela 12, 13071 Ciudad Real, Spain

^c Instituto de Energías Renovables, Universidad de Castilla-La Mancha (UCLM), Paseo de la Investigación 1, 02006 Albacete, Spain

^d Department of Chemical Engineering, University of Patras, 1 Carathéodory St, GR-26504 Patras, Greece

ARTICLE INFO

Article history:

Received 15 June 2012

Received in revised form 25 October 2012

Accepted 1 November 2012

Available online 29 November 2012

Keywords:

Methane oxidation

Electrochemical promotion

NEMCA

Pd catalyst-electrode

Porous YSZ

ABSTRACT

The aim of the present study was to explore the potential to electrochemically promote the methane oxidation reaction over palladium catalyst-electrodes deposited on a combination of porous-dense Y_2O_3 -stabilized- ZrO_2 (YSZ), an oxygen ion conductor. We have prepared for the first time an electro-active palladium catalyst on a highly porous support, which was successfully used to enhance the catalytic activity by electrochemical promotion (NEMCA effect or EPOC). The wet impregnation technique has been used over highly porous YSZ disks to achieve very active catalyst-electrodes, with a metal catalyst dispersion of 27% (up to 4.5 times higher than that obtained for catalysts supported on dense YSZ), and susceptible to be electropromoted, despite its relatively high in-plane electrical resistance. The sample impregnated on porous YSZ turned to be much more active in methane combustion than the sample prepared by impregnation on dense YSZ, reaching, under similar working conditions, one order of magnitude higher CO_2 formation rates. The catalyst supported on porous YSZ was characterized by XRD, XPS, SEM and TEM techniques, while galvanostatic transients and electrochemical current-potential curves were recorded in order to assess the electropromotion of the catalytic reaction in a temperature range from 350 to 430 °C under reducing, stoichiometric and oxidizing conditions.

© 2012 Elsevier B.V. All rights reserved.

1. Introduction

Methane is a greenhouse gas estimated to have a 20-year global warming potential 35 times larger than that of carbon dioxide at equivalent emission rates. Therefore, it is important to reduce the amounts emitted into the atmosphere to mitigate in the short term the global warming. Catalytic combustion of methane, which is the main component of natural gas, is of actual interest both as a means for generating power with minimal formation of NO_x , and as a means for removing small amounts of methane from emissions of methane-burning engines [1,2]. Thus, on one hand, catalytic combustion of natural gas is being vigorously explored as a route to production of heat and energy in view of its capability to achieve effective combustion at much lower temperatures than in conventional flame combustion, hence allowing lower emissions [3,4]. On the other hand, lean burn natural gas vehicles (NGVs) are now commercially available in service vehicles as a viable approach to

meet particulate and gaseous emission standards in urban environment in United States and Europe. However, methane is the main hydrocarbon species emitted by these vehicles, so development of efficient catalysts is needed to approach methane emissions control from NGVs [5,6].

Several effective combustion catalysts have been developed so far. They can be divided in two main categories: mixed metal oxides, and noble metals. Higher catalytic activity per site and greater resistance to sulfur poisoning are the main advantages of noble metal catalysts over metal-oxide catalysts [7]. Among the noble metal catalysts, supported Pd has been widely reported as the catalyst of choice for methane combustion applications [8–10]. It has been reported that the catalytic activity for the methane combustion depends strongly on the chemical state of palladium. It is commonly accepted that at low temperature the active phase is crystalline PdO , which may exist in more than one form depending on the oxidized particles size and on the nature of the support, but at high temperature metallic Pd is the active phase for methane oxidation [11–15].

Since the active phase, in the case of noble metals, is quite expensive, it is rather advantageous to prepare catalysts with high dispersions. This can be usually accomplished by the preparation of the catalyst as well as the calcination process. The support has

* Corresponding author. Tel.: +30 2610 997576; fax: +30 2610 997269.

** Corresponding author. Tel.: +40 244 573 171; fax: +40 244 575 847.

E-mail addresses: brosda@chemeng.upatras.gr (S. Brosda),

dciuparu@upg-ploiesti.ro (D. Ciuparu).

an important role in the metal dispersion since the maximization of the surface area could provide a large area over which it may be spread, thus providing larger active surface. Additionally, the support may act as a stabilizer of the active phase and, in some cases even, may be involved in the catalytic reaction [16].

Alumina and zirconia are the most studied supports for palladium catalysts in the methane oxidation reaction, but other supports have also been observed to improve the catalytic performance. For the Pd/alumina system, Baldwin and Burch [17] observed that the catalysts supported on δ -alumina were significantly more active than catalysts supported on γ -alumina. However, instead of attributing this to a support effect, the authors related the effect to the difference in morphology of Pd on different supports. Cullis and Willat [18] tested titania, thoria, and tin oxide, and found that Pd on these supports was less active for methane oxidation than when supported on alumina. Ribeiro et al. [19] demonstrated that Pd/ZrO₂ leads to a higher reaction rate than Pd/Al₂O₃. Sekizawa et al. [20] showed that Pd-supported on monoclinic ZrO₂ was more active than that on tetragonal ZrO₂. Interestingly, Escandón et al. [21] demonstrated that zirconia-based supports present high stability, especially in the case of the yttrium-doped support. Furthermore, many investigators have shown that the oxidation/reduction behavior of supported Pd catalysts can be strongly affected by metal-support interactions [9,16,22]. In brief, it has been demonstrated that the choice of the support can clearly affect the Pd–PdO transformations that are important for methane combustion since the catalytic activity strongly depends on the palladium oxidation state.

During the last years, the possibility of enhancing the catalytic activity by applying small currents or potentials between a catalyst (which serves also as the working electrode) supported on a solid electrolyte, and a counter electrode also supported on the same electrolyte, has been investigated. This phenomenon, introduced first by the group of Prof. Vayenas in the early 1980s [23,24], is called electrochemical promotion of catalysis (EPOC) or non-Faradaic electrochemical modification of catalytic activity (NEMCA) and originates from the controlled migration of promoting species from the electrolyte support to the catalytic metal/gas interface during polarization. These backspillover ionic species form an overall neutral double layer at the metal/gas interface and affect catalytic rates by modifying the catalyst work function, i.e. the binding energy of chemisorbed reactants and intermediates primarily via lateral electrostatic interactions [25,26]. Thus, it was shown conclusively that electrochemical promotion is an electrically controlled metal–support interaction and at least certain types of metal–support interactions are induced by reverse spillover of promoter species from the solid electrolyte onto the surface of the catalyst-electrode [27].

This phenomenon has been studied for a wide variety of catalytic reactions including methane oxidation on Rh [28,29], Pt [30] and Pd catalyst-electrodes [31–34]. In these systems dense pellets of Y₂O₃-stabilized-ZrO₂ (YSZ), with O²⁻ conductivity have been used as the solid electrolyte. In the majority of these studies, porous pasted catalytic films were used [25]. However, recently, it has been demonstrated that the wet-impregnation procedure is a suitable and simple technique for preparing thin catalyst-electrode films [35–37]. Besides, in the last years, there have also been reported new routes to improve the metal–support interactions and to increase the dispersion of the metal particles in NEMCA electrodes. For instance, it has been investigated the use of an interlayer between the catalytic film and the YSZ dense electrolyte support such as CeO₂ [38,39] or TiO₂ [40]. It was found that the enhancement in the catalytic activity was due to the increase in metal dispersion, and the improvement in the magnitude of the electrochemical promotion was mainly influenced by the mixed ionic-electronic conductivity of the interlayer. Moreover, Jiménez

et al. [41] prepared composite electrodes based on Ni or Ru impregnated CNF (carbon nanofibers) with dispersions of up to 7% that were successfully applied for electropromoting the CO₂ hydrogenation reaction. Also, De Lucas-Consuegra et al. [42] found that the addition of some YSZ powder to the platinum paste ink led to the decrease of the metal particle size, thus stabilizing higher dispersion.

The aim of this work was to prepare Pd catalytic films interfaced with either highly porous or dense YSZ and to comparatively investigate their electrochemical promotion for methane oxidation under reducing, stoichiometric and oxidizing conditions. The catalytic experiments were complemented with different characterization techniques, which provided useful insights in the intimate mechanisms governing the performance of these types of catalytic systems.

2. Experimental

The catalyst-electrodes used in this work consisted of a palladium film deposited on either dense or porous solid electrolyte pellets, i.e. 8 mol% Y₂O₃-stabilized ZrO₂ (YSZ). Fully dense YSZ disks (19 mm diameter and 1 mm thickness) were prepared after pressing commercial YSZ powders (Pi-KEM) at 1 ton and sintering at 1500 °C for 24 h. As prepared dense disk were used to prepare the catalysts used as the reference material for the dense catalyst in one experimental run.

For the preparation of the Pd catalyst on porous YSZ, a porous YSZ interlayer was deposited on a dense YSZ disk, prepared as described above. The porous layer was prepared by mixing YSZ powder with an organic binder (Decoflux, Zschwimmer and Schwartz) in a 1:1 (w/w) ratio and spin-coating on one side of the dense electrolyte. The assembly was dried at 100 °C for 1 h in an oven and then calcined at 1000 °C for 6 h to ensure good adherence.

The solid electrolyte disk was covered by three electrodes: working, counter and reference. Inert gold counter and reference electrodes were deposited on the dense side of the solid electrolyte by application of thin coatings of gold paste (Metalor, A1118) followed by calcination in air for 30 min at 450 °C and for 60 min at 650 °C.

The Pd catalytic film, serving as the working electrode, was deposited on the porous side of the disk, opposite to the counter electrode. The Pd film was prepared by an impregnation technique consisting of successive steps of deposition and thermal decomposition of the aqueous solution of 0.1 M [Pd(NH₃)₄](NO₃)₂ Pd precursor. Initially, 20 μ L of precursor solution were deposited on the YSZ substrate using a plastic circular mask in order to obtain a 2.01 cm² geometric surface area of the catalytic film. Then, evaporation of the solvent took place at 70 °C for 10 min, followed by drying of the sample at 120 °C overnight and then calcination at 450 °C for 2 h. Several successive steps of this deposition procedure followed by drying and heating were repeated until a final metal loading of 0.85 mg Pd was obtained. The active area of the catalyst-electrode film was determined by the electrochemical technique developed by Ladas et al. [43] and it was found to be 64 cm² for the Pd catalyst supported on dense YSZ, and 345 cm² for the Pd catalyst supported on porous YSZ. Considering the atomic density of PdO (101), 2.75×10^{-20} m² atom⁻¹ [44], the resulting dispersions are 4.9 and 27% for the catalyst supported on dense, and porous YSZ, respectively.

The structure and morphology characterization of the fresh catalytic layers were carried out by scanning electron microscopy (SEM) using a JEOL JSM-6300 microscope. Fresh Pd films were also imaged by transmission electron microscopy (TEM) using a JEOL 2100 microscope. The crystalline phases of the palladium catalysts supported on the porous electrolyte were examined by X-ray powder diffraction (XRD) performed using a PANalytical diffractometer

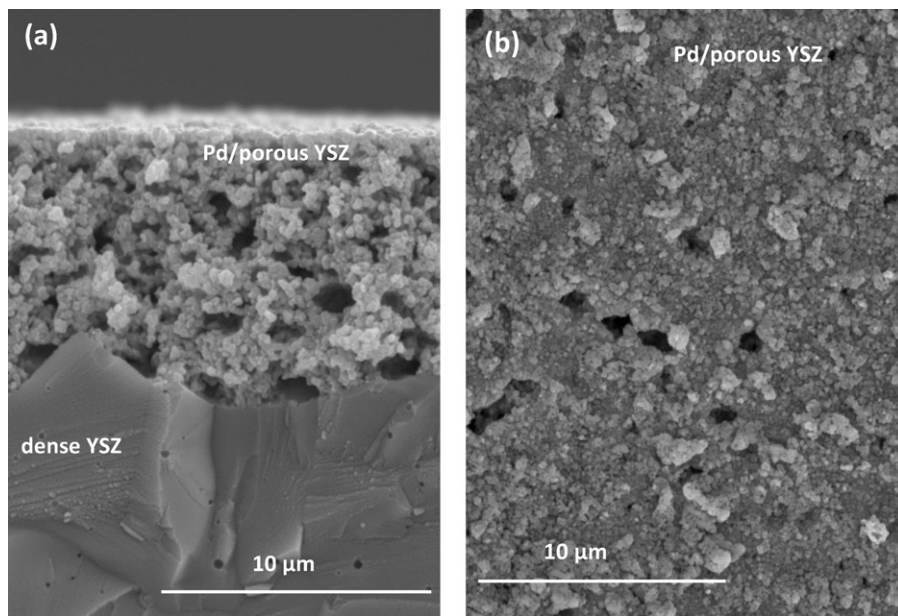


Fig. 1. SEM images of the Pd catalyst deposited on porous YSZ: (a) cross section and (b) top view.

with monochromatic Cu K α 1 radiation ($\lambda = 1.54 \text{ \AA}$) equipped with an X'Celerator detector. Scans were collected in the 2θ range from 20° to 80° and the crystal planes of the deposited films were identified according to JCPDS crystallographic database. The X-ray photoelectron spectra (XPS) were recorded on a K-Alpha (Thermo Scientific) spectrometer, equipped with a double focusing hemispherical analyzer and an aluminum anode (Al K = 1486.6 eV). The residual pressure in the analysis chamber was $2 \times 10^{-9} \text{ mbar}$. Also, an ion bombardment with a 1 keV Ar $^+$ beam gun was carried out in order to study the depth-profile surface of samples showing peaks with binding energies shifted from regular values corresponding to either metallic or fully oxidized palladium. Samples were placed on metal holders and the recording conditions for the spectra and the data processing were identical for all analyzed samples. Data were collected using a computer interface and then digitally smoothed.

The reaction experiments were carried out within a continuous flow, atmospheric pressure quartz reactor (single chamber) of 30 cm^3 volume, described in detail elsewhere [25,34]. Reactants were Messer–Griesheim certified standards of 5.6% CH₄ in He and 20% O₂ in He. These mixtures could be further diluted in ultra-pure (99.999%) He (L'Air Liquide). Gas flow rates were maintained using Brook mass flow controllers connected to a 4-channel Brose control box (model 5878). The feed gas composition depended on the experiment. CH₄ and O₂ partial pressures were held constant at $P_{\text{CH}_4}/P_{\text{O}_2} = 2.9 \text{ kPa}/1.9 \text{ kPa}$, $P_{\text{CH}_4}/P_{\text{O}_2} = 1.4 \text{ kPa}/2.8 \text{ kPa}$, and $P_{\text{CH}_4}/P_{\text{O}_2} = 1.3 \text{ kPa}/4.5 \text{ kPa}$ for reducing, stoichiometric and oxidizing conditions, respectively. The total flow rate in all the experiments was $200 \text{ cm}^3 \text{ min}^{-1}$ (STP).

Both samples supported on dense electrolyte and on porous YSZ interlayer, respectively, have been exposed to a complete set of tests consisting of oxidative, stoichiometric and reducing atmosphere activity measurements. The first experiments carried out consisted of a set of light off curves, in oxidizing gas mixture, described in detail elsewhere [39,45]. After light off, the samples were cooled down to room temperature, only in the gas carrier, i.e. He. Subsequently, in order to assess the electropromotion of the catalytic reaction, galvanostatic transients and electrochemical current–potential curves have been recorded at three different temperatures, 350 °C, 400 °C and 430 °C, under oxidizing, stoichiometric and reducing conditions – in this precise sequence for each

temperature. Samples after this series of tests are further referred to as “used samples”.

A four-port valve was used in order to lead the gas supply either directly to the analysis unit, or to the reactor and then to the analysis unit. The reaction temperature was monitored via a K-type thermocouple placed inside the quartz tube, and controlled via a JUMO (iTRON 08) temperature controller.

Analysis of the reactants and products was performed using online gas chromatography (Hewlett Packard 5890 Series II), while an infrared analyzer (Rosemount Binos 100) was used for the continuous and quantitative measurement of the CO₂ concentration. The gas chromatograph is equipped with a Thermal Conductivity Detector (TCD) and two columns, a Molecular Sieve 5A (for the separation of O₂, CH₄ and CO) and a Porapak Q column (for the separation of CH₄ and CO₂). TCD signals were integrated and recorded on line by the use of a Hewlett Packard integrator (model 3395).

Application of constant currents or potentials was carried out with a SOLARTRON electrochemical interface 1286. During catalytic activity measurements, the in-plane resistance of the catalyst film was monitored. For this purpose the catalyst-electrode (working electrode) was connected to two point contacts (Au wires) placed at 8 mm distance from each other. The ohmic resistance between these two points was obtained with a Digital Multimeter (Mastech MY-68) during light off experiments and only under open circuit conditions [39].

The contributions of homogeneous reaction as well, as the catalytic rate of methane combustion on both the pure solid electrolyte and gold electrodes were found to be negligible under the operating conditions used. Thus, all the catalytic activity should be exclusively attributed to palladium. Carbon dioxide was the only carbon-containing product since CO and other carbon based compounds were never detected.

3. Results and discussion

3.1. Catalyst-electrode characterization

The porous YSZ layer deposited by spin coating on the dense YSZ disk was approximately 12.5 μm thick, as highlighted in Fig. 1a. Higher resolution images revealed good contact between

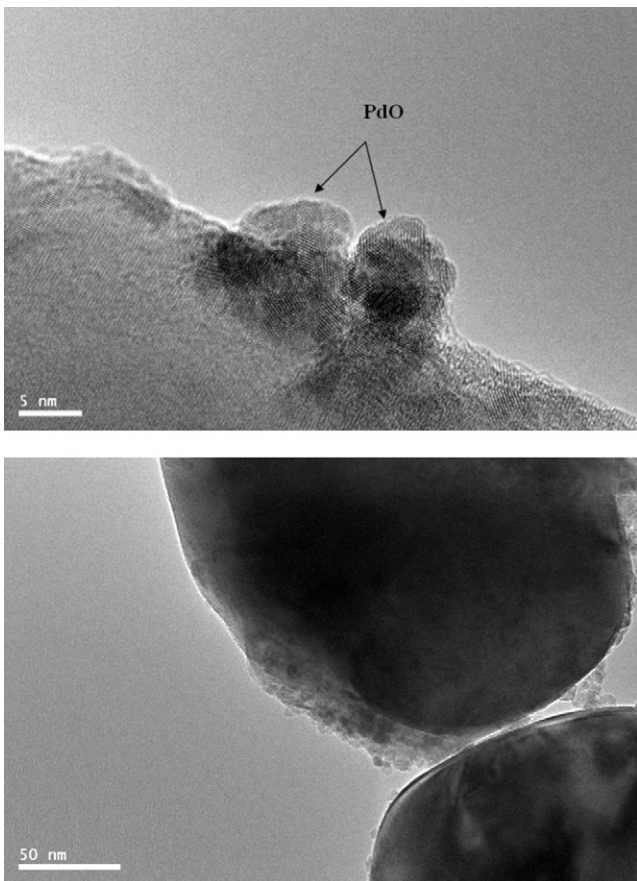


Fig. 2. TEM images of the Pd catalyst deposited on porous YSZ: (a) high resolution image of PdO particles with lattice spacing details and (b) morphology of dispersed PdO particles on the porous electrolyte.

the porous layer and the dense electrolyte. No cracks or delimitations of the porous layer were observed after preparation. On the other hand, the top view of the assembly (Fig. 1b) shows a fairly high porosity with rather uniform distribution regarding the number and pore sizes.

Transmission electron microscopy (TEM) was used to image the catalyst structure and palladium dispersion on the fresh, as prepared catalyst. The PdO particles are easily identified, visible as small darker spots (see arrows in Fig. 2a) on the porous YSZ support. The particle size observed in TEM micrographs is approximately 8 nm and Fig. 2b suggests a rather homogeneous distribution of PdO particles on the porous YSZ.

Fig. 3 shows the XRD patterns of the palladium catalyst-electrode deposited on porous YSZ. Diffractograms of both fresh (catalytic film as prepared) and used (catalytic film after exposure to a complete set of tests consisting of oxidative, stoichiometric and reducing atmosphere activity measurements) samples are shown in order to observe the influence of the exposure to the reaction conditions on the palladium phase.

Regarding the solid electrolyte, the characteristic peaks of YSZ are observed, $Zr_{0.8}Y_{0.2}O_{1.9}$ (JCPDS-ICDD Card No. 01-082-1246), corresponding, mainly, to the (1 1 1), (2 0 0), (2 2 0), (3 1 1), (2 2 2) and (4 0 0) planes. For the fresh catalyst, there were also observed peaks corresponding to palladium oxide (JCPDS-ICDD Card No. 41-1107) with tetragonal structure where reflections appear at 33.8° , 41.9° , 54.7° and 71.2° corresponding, respectively, to the (1 0 1), (1 1 0), (1 1 2) and (2 0 2) planes of PdO. However, for the used sample, both phases – palladium oxide and metallic palladium – were observed, the latter consistent with a face-centered cubic (fcc)

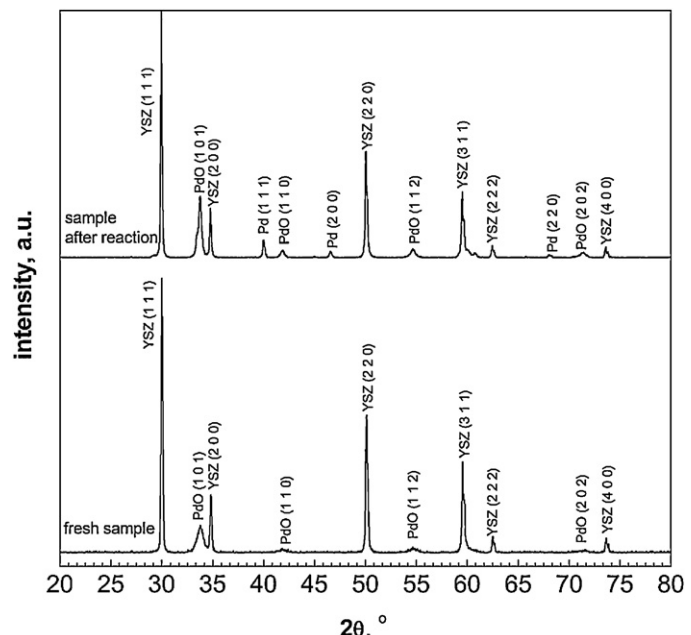


Fig. 3. XRD patterns of the Pd catalyst deposited on porous YSZ before and after exposure to reaction conditions.

structure where reflections appearing at 40.1° , 46.6° and 68.1° correspond, respectively, to the (1 1 1), (2 0 0) and (2 2 0) planes of Pd^0 (JCPDS-ICDD Card No. 05-0681).

The presence of only palladium oxide in the fresh sample is due to the preparation process of the catalyst film at a relatively low calcination temperature (450°C), in the presence of air, since the transition from PdO to Pd^0 , in air, for Pd dispersed catalysts on YSZ takes place at around 600°C [6]. Furthermore, the use of ammonic nitrate solution as precursor favors the oxide formation when the nitrates are decomposed during the calcination process. After the Pd film has been exposed to a complete set of tests as discussed in Section 2, at temperatures not exceeding 450°C , the catalyst shows the co-existence of both palladium phases. This observation strongly suggests that during the methane oxidation reaction some partial reduction of the PdO phase occurs.

In previous work with similar Pd catalyst-electrodes, but deposited on dense YSZ [34,45] and on CeO_2/YSZ [39], it was also found that the as-prepared catalytic film only exhibited the oxide palladium phase. This can be explained since the same catalyst preparation process was used. In the case of the used catalyst, it was observed that when it is deposited on dense YSZ only the metallic palladium phase was obtained on samples following an identical set of experiments [45]. However, Pd impregnated on CeO_2/YSZ exhibited both palladium phases [39]. This was explained on the grounds of the oxygen storage capacity of ceria, which leads to the stabilization of some PdO phase. In the present case, the YSZ porous interlayer has a similar effect as the CeO_2 interlayer, since its high porosity and better dispersion ensures a more intimate contact between the porous YSZ and the PdO phases, enabling the oxygen exchange between phases and stabilizing the PdO phase.

X-ray diffraction can be also used to estimate the crystallite size of catalyst particles [46]. For both fresh and used porous interlayered samples, the crystallite size was calculated using the Debye-Scherrer equation [47], which allows estimating the particle size with a reasonable accuracy.

$$D = \frac{0.9\vartheta_{\text{Cu}}}{\beta_{1/2} \cos \theta} \quad (1)$$

Table 1

XPS analysis of the Pd catalyst deposited on porous YSZ.

Pd impregnated on porous YSZ	Binding energy, eV		XRD phase analysis
	PdO	Pd ⁰	
Fresh sample	337.4	342.8	—
Used sample	337.1	342.4	— PdO, Pd ⁰

where ϑ_{Cu} is the X-ray wavelength, $\beta_{1/2}$ is the line broadening at half maximum intensity (FWHM) in radians, and θ is the Bragg angle.

In the fresh porous YSZ interlayered sample, the average crystallite size for PdO is 10.8 nm, in a rather fair agreement with the particle size estimated from TEM, i.e. 8 nm. Meanwhile, for the used sample the PdO crystallite size is increasing to 29 nm and the Pd crystallite size was calculated to be 20 nm. From the values of the particle size calculated using Scherrer equation, dispersion has been estimated at a value of approximately 30% for the fresh impregnated sample on the porous interlayered electrolyte. Taking into account the tetragonal structure of PdO and considering a hemispherical shape of the PdO crystallite, the dispersion has been calculated as the ratio between the number of the PdO crystalline cells exposed to the gas mixture and the total number of PdO crystalline cells within the catalyst film consisting of crystallites of 10.8 nm in size. This value of the dispersion is in good agreement with the one estimated using the electrochemical technique developed by Ladas et al. [43], i.e. 27% as discussed above.

Surface characterization of the palladium film deposited on porous YSZ was carried out using X-ray photoelectron spectroscopy (XPS). Binding energy results are presented in Table 1 along with XRD findings, for comparison. As in the case of XRD, the XPS spectra of the fresh (Pd film as prepared) and the used sample (Pd film after exposure to reaction conditions) are compared in Fig. 4.

The XPS spectra in Fig. 4a show the presence of PdO on the surface of the fresh sample, also confirmed by the XRD analysis, which showed just the PdO phase to be present in this sample. However, for the used sample, there is an apparent disagreement between the XRD and XPS results. Bulk analysis (Fig. 3) showed that both PdO and Pd metallic were present in this sample, while surface analysis (Fig. 4a) showed peaks only for PdO, although a slight shift of the binding energies toward lower values can be noticed in the spectrum of the used sample in Fig. 4a. These results suggest that the oxide surface is covering metallic Pd particles formed on the electrolyte disk, and that the thickness of the oxide layer is larger than 5 nm, not allowing the detection of the Pd metallic phase by XPS. The hypothesis of an oxide layer over metallic Pd particles is supported by the fact that the binding energy value is shifting toward lower values, which correspond to metallic Pd phase. The oxide layer covering a metal core has been previously proposed in the literature [48]. Therefore, even though the metallic Pd phase was not shown by surface characterization, the shifting of the XPS peak toward lower values, in combination with the XRD results, suggests the existence of metallic Pd particles covered by a thick PdO layer.

Moreover, a depth profile analysis has been further performed in the attempt to validate the hypothesis of an oxide layer covering the metallic Pd particles. To this end, an Ar⁺ beam gun has been used to achieve surface erosion by emission of secondary particles from the surface. By continuous sputtering, layers beneath the original surface were subsequently exposed and analyzed. Thus, an in-depth distribution as a function of the sputtering time is showed in Fig. 4b. As it can be observed, even after 30 s bombardment with argon ions, the Pd 3d_{5/2} peak reached a significantly lower value of the binding energy, 335.5 eV. The newly obtained value of the binding energies are slightly higher than those reported in the literature for high-dispersion surface Pd metallic, i.e. 334.5 eV [49]; however,

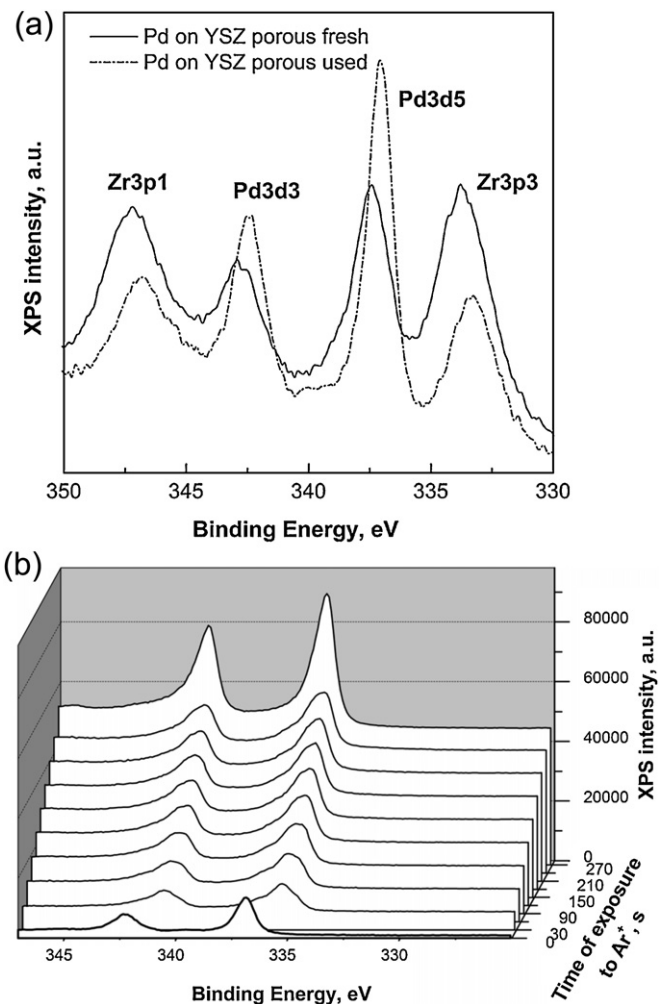


Fig. 4. (a) XPS spectra of the Pd catalyst deposited on porous YSZ before (solid line) and after exposure to reaction conditions (dash line). (b) Depth-profile XPS spectrum for the porous interlayered used sample. The profiles were obtained using 1 keV Ar⁺ sputtering times of 30, 60, 90, 120, 150, 180, 210, 240 and 270 s.

further exposure to Ar⁺ ions during the depth profiling analysis results in further shifting of the binding energy toward lower values – 335.0 eV after 270 s bombardment – along with the increase in the signal intensity, confirming the increase in the flux of emitted photoelectrons corresponding to the more pronounced metallic character of the bulk layers in the catalyst particles. This behavior confirms the results obtained by XRD measurements indicating both palladium phases are present in the used porous interlayered sample.

3.2. Catalytic activity under open-circuit conditions

Fig. 5 shows the catalytic CO₂ production rate and the in-plane resistance of the catalytic film as functions of the reaction temperature, under oxidizing reaction conditions, for the catalysts supported on dense and porous electrolytes. For both catalysts the ignition took place at the same temperature, around 270 °C. However, the catalytic activity was significantly affected by the porosity of the support: the Pd catalyst supported on porous YSZ was more active than the catalyst deposited on dense YSZ. Thus, at 400 °C, CO₂ formation rates of 2.9×10^{-7} and 23×10^{-7} mol O/s were found for Pd on dense, and on porous YSZ, respectively. The CO₂ formation rate is almost one order of magnitude higher and this can be explained by the better palladium dispersion obtained for the

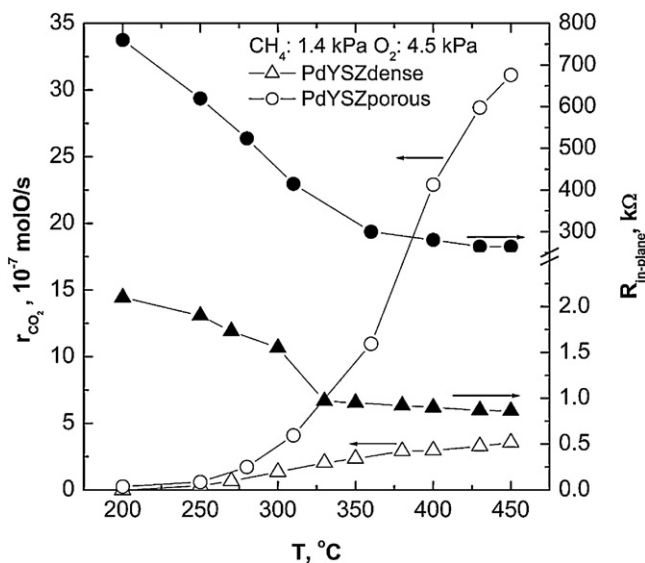


Fig. 5. Effect of the temperature on methane conversion, CO_2 formation rate and in-plane resistance of the Pd catalyst deposited on dense and on porous YSZ. Conditions: $P_{\text{CH}_4} = 1.2 \text{ kPa}$, $P_{\text{O}_2} = 4.5 \text{ kPa}$, $F = 200 \text{ ml/min}$.

porous supports, which was found to be approximately 4.5 times higher than that of the catalyst supported on dense YSZ.

The palladium distribution on the support also strongly affected the in-plane resistance of the working electrode (Fig. 5). When palladium is supported on porous YSZ, the measured in-plane resistance is two orders of magnitude higher than that for Pd deposited on dense YSZ. The important decrease of the in-plane resistance with the temperature increase for both catalysts, besides the improvement of the film conductivity caused by the temperature, can be related to the formation of metallic palladium during the reaction since PdO shows much higher bulk and surface resistance than Pd metallic [50]. This is consistent with the co-existence of the two phases, reduced and oxidized, on the used catalyst sample identified by XRD, and suggested by XPS. Apparently, reduction of the PdO phase is a fast process taking place at the light off temperature, while reoxidation is slower and, thus, incomplete during reaction, leaving the metal core of the particle with higher in plane electrical conductivity, as indicated by the in-plane resistance measurements.

3.3. Electrochemically promoted catalytic activity

The application of currents or potentials to the catalyst and its influence on the catalytic activity of Pd deposited on porous YSZ catalyst was studied under reducing, stoichiometric and oxidizing conditions, at temperatures ranging from 350 to 430 °C. The quantitative description of the promoting effect can be based on two main parameters commonly used to quantify the magnitude of the NEMCA phenomenon [25]:

(a) the rate enhancement ratio (ρ), defined by Eq. (2):

$$\rho = \frac{r}{r^0} \quad (2)$$

where r^0 is the catalytic rate at open circuit and r the catalytic rate under polarization conditions; and

(b) the apparent Faradaic efficiency, Λ , defined by Eq. (3):

$$\Lambda = \frac{r - r^0}{I/2F} \quad (3)$$

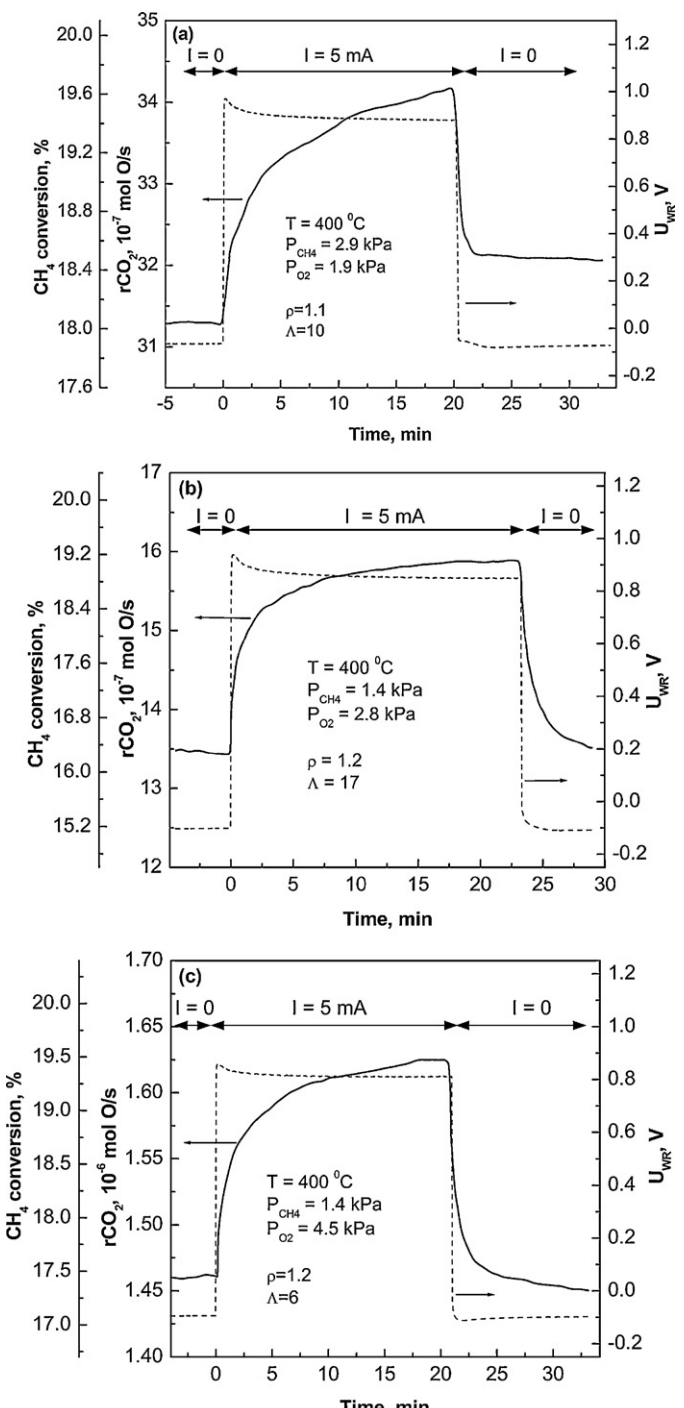


Fig. 6. Transient response of the CO_2 formation rate, methane conversion and of the catalyst potential upon application of a current $I = +5 \text{ mA}$ under (a) reducing, (b) stoichiometric and (c) oxidizing conditions of the Pd catalyst deposited on porous YSZ.

where I is the applied current, F is the Faraday constant, and $I/2F$ equals the rate of O_2^- supply to the catalyst.

Fig. 6a shows the transient effect of a constant positive current application (+5 mA) between the catalyst-electrode and the Au counter electrode on the catalytic CO_2 formation rate and on the methane conversion, as well as on the potential between the working and reference electrodes, under reducing conditions ($\text{CH}_4/\text{O}_2: 2.9\%/1.9\%$). Initially, at $t < 0$, under open-circuit conditions, the unpromoted catalytic rate, r^0 , was found to be equal

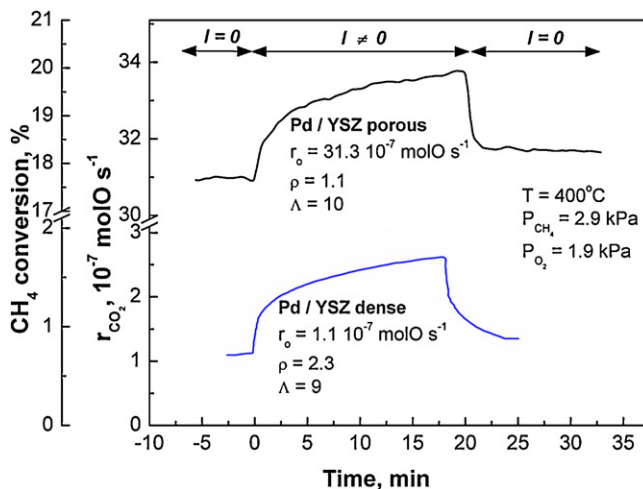


Fig. 7. Transient response of the CO_2 formation rate and methane conversion upon anodic polarization for samples supported on dense electrolyte and porous YSZ interlayer, respectively.

to $31.3 \times 10^{-7} \text{ mol O s}^{-1}$. At $t=0$, the positive current application for 20 min caused an increase in the catalytic CO_2 formation rate until the new value of r , $34.1 \times 10^{-7} \text{ mol O s}^{-1}$ has stabilized. Due to the current application, oxygen ions, O^{2-} , are transferred from the YSZ support to the Pd catalyst-electrode at the rate $I/2F$ equal to $2.59 \times 10^{-8} \text{ mol O s}^{-1}$. The increase in the catalytic rate, Δr , of $2.8 \times 10^{-7} \text{ mol O s}^{-1}$, is 10 times larger than the rate of ion transport, $I/2F$. This implies that each O^{2-} supplied to the Pd catalyst surface causes 10 chemisorbed O atoms to react with methane. The two parameters, rate enhancement and Faradaic efficiency, were 1.1 and 10, respectively.

Fig. 6b shows a similar catalytic activity transient response of the catalytic activity upon constant anodic applied current (+5 mA), but under stoichiometric conditions (CH_4/O_2 : 1.4%/2.8%). In that case, the CO_2 formation rate has increased with a rate enhancement ratio of $\rho = 1.2$ and a Faradaic efficiency, Λ , of 17.

In Fig. 6c is shown the galvanostatic transient of the catalytic activity under oxidizing conditions (CH_4/O_2 : 1.4%/4.5%) upon the same value of constant applied positive current (+5 mA). Similarly with the two cases discussed above, upon positive current application, up to 20% increase of the catalytic rate was observed, while the apparent Faradaic efficiency was 6. Despite its high intrinsic activity and in plane resistance, this new type of electrode can still be electrochemically promoted. Under reducing conditions, the recorded open circuit CO_2 formation rate value is higher than those recorded while working under oxidation and stoichiometric conditions. Similar behavior was also reported in methane oxidation on Rh catalyst [28] and was attributed to the kinetics of methane oxidation reaction on Rh catalysts, i.e. the competitive adsorption of CH_4 on a catalytic surface with higher oxygen coverage.

While working under anodic polarization, higher values of one or even both NEMCA parameters are obtained under oxidizing and stoichiometric conditions compared to the one recorded for reducing conditions. Such behavior was never reported in the literature, to the best of our knowledge, for Pd catalysts supported on dense YSZ and can be rationalized on the basis of the kinetics of methane oxidation on Pd based catalysts. Under fuel lean feed stream, methane oxidation rate is first order in CH_4 and zero order with respect to oxygen [32], which implies that the catalytic surface is covered with oxygen, thus the rate limiting step is the reaction of the chemisorbed oxygen with methane, i.e. the competitive adsorption of methane on an oxygen-covered surface. Working under stoichiometric conditions lowers the oxygen concentration, but yet maintains the surface catalyst covered with oxygen. Under

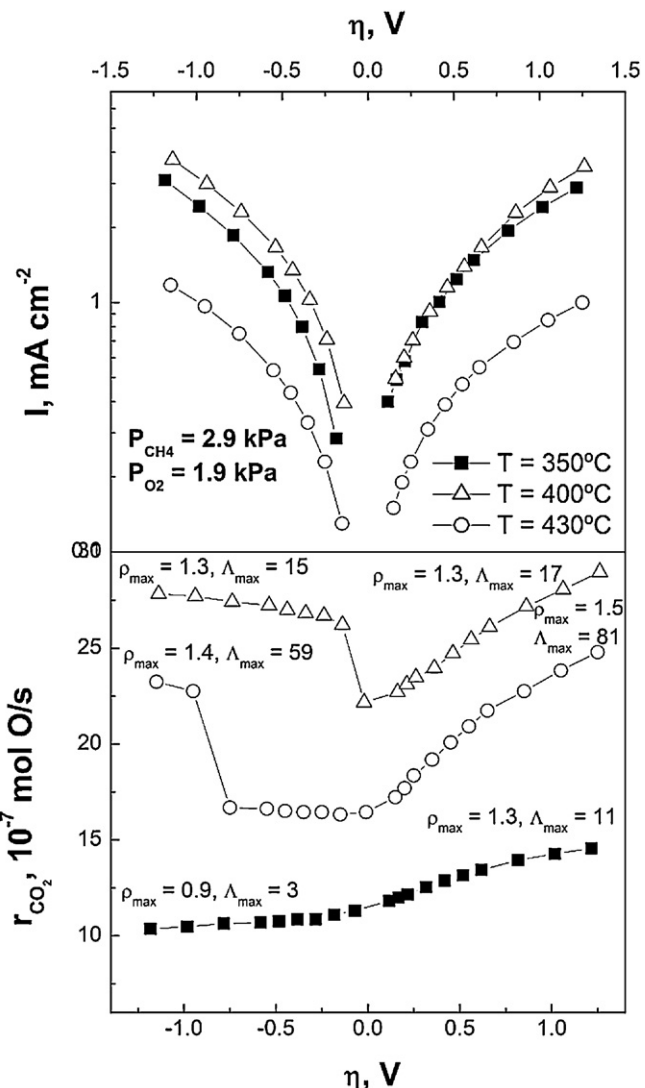


Fig. 8. Effect of the applied potential and temperature on the electrochemically promoted methane oxidation on the Pd catalyst deposited on porous YSZ. Top: Tafel plot and bottom: CO_2 formation rate. Conditions: $P_{\text{CH}_4} = 2.9 \text{ kPa}$, $P_{\text{O}_2} = 1.9 \text{ kPa}$, $F = 200 \text{ ml/min}$.

fuel rich conditions, however, an insufficient amount of oxygen is adsorbed on the catalytic surface, so the rate-limiting step becomes the adsorption of O_2 from the gas phase. Thus, under stoichiometric and oxidation conditions, the active adsorbed oxygen on the catalytic surface is more abundant than in fuel rich conditions, leading to higher ρ values. The higher Λ value registered under stoichiometric conditions might be explained on the basis of the back-spillover oxide ions, which migrate from the porous YSZ onto the catalyst surface under the influence of current application [25].

In our previous work [39], under identical reaction conditions, but using a Pd catalyst at the same metal loading supported on dense YSZ, we have observed a lower catalytic activity, i.e. the r^0 was found to be equal to $1.9 \times 10^{-7} \text{ mol O/s}$ for the impregnated sample on dense YSZ, while for the porous YSZ sample discussed in this study the rate under open circuit conditions is equal to $14.6 \times 10^{-7} \text{ mol O/s}$. This is consistent with the results presented in Fig. 5, which show that, under open circuit conditions, the CO_2 formation rate is higher for the porous YSZ sample than for the dense YSZ. In [39], upon positive current application, the CO_2 formation rate increased with a rate enhancement ratio ρ of 1.7 and a Faradaic efficiency, Λ , of 63. The values of the two main parameters

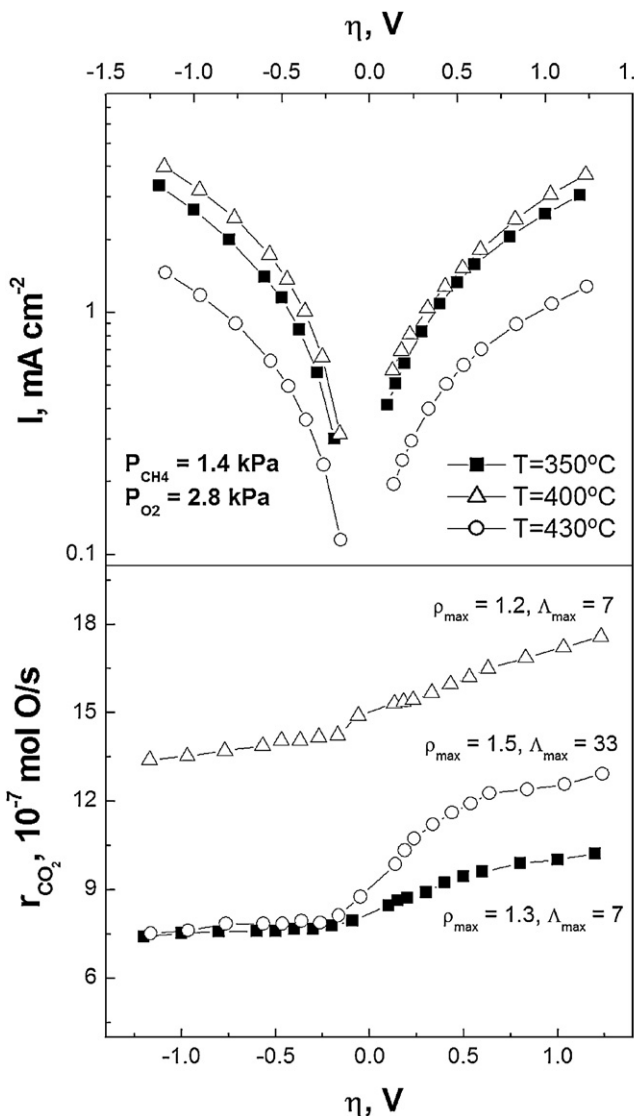


Fig. 9. Effect of the applied potential and temperature on the electrochemically promoted methane oxidation on the Pd catalyst deposited on porous YSZ. Top: Tafel plot and bottom: CO_2 formation rate. Conditions: $P_{\text{CH}_4} = 1.4 \text{ kPa}$, $P_{\text{O}_2} = 2.8 \text{ kPa}$, $F = 200 \text{ ml/min}$.

used to quantify the magnitude of the NEMCA effect are slightly higher in the case of the sample impregnated on dense YSZ, but even after electropromotion, the obtained catalytic rate is lower for the impregnated sample on dense YSZ, than for that recorded in the case of the sample impregnated on porous YSZ. This can be seen in Fig. 7 that shows a comparison between two galvanostatic transients performed on impregnated catalyst-electrode on both dense and respectively on porous interlayered electrolyte. Comparing the behavior of samples supported on dense and porous interlayer electrolytes, one can observe that under anodic polarization the increase in the CO_2 formation rate is similar in absolute values, which is a quite seldom effect for catalysts with high intrinsic activity.

The behavior observed during the galvanostatic transients (Fig. 6a–c) suggests that under anodic polarization an increase in the oxygen coverage of the catalyst film also leads to a reaction rate increase. Therefore, the back-spillover of electron acceptor species (O_{ads}) led to an increase in the catalyst work function and, hence, to an enhancement of the chemisorptive bond of electron donor adsorbates (methane). Thus, the increase in the CO_2 formation rate

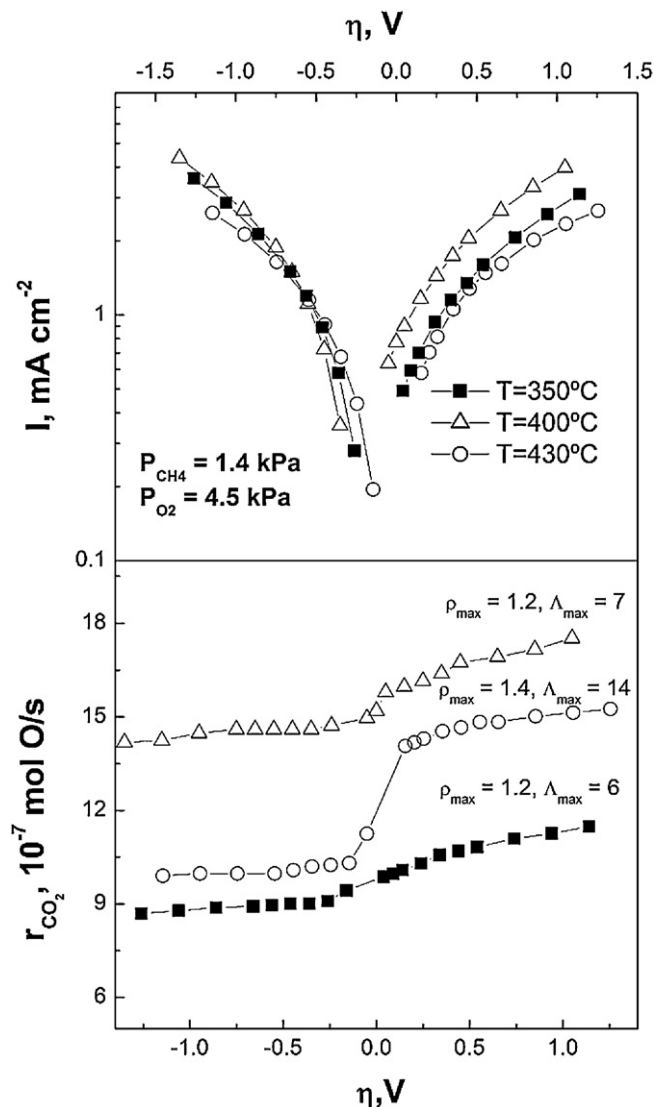


Fig. 10. Effect of the applied potential and temperature on the electrochemically promoted methane oxidation on the Pd catalyst deposited on porous YSZ. Top: Tafel plot and bottom: CO_2 formation rate. Conditions: $P_{\text{CH}_4} = 1.4 \text{ kPa}$, $P_{\text{O}_2} = 4.5 \text{ kPa}$, $F = 200 \text{ ml/min}$.

upon positive polarization can be attributed to weakening of the Pd–O bond, due to the increase of the catalyst work function, which causes a decrease in the oxygen coverage of the catalytic surface. Consequently, the catalytic reaction rate has increased by anodic polarization, exhibiting electrophobic behavior [25]. This is in good agreement with the literature reports [28–34], where the methane oxidation reaction has always been found to be electrophobic, independent on the catalytic system studied.

It is worth to note that, after current interruption, the catalytic rate reversibly returns to its initial steady-state value only under oxidizing and stoichiometric conditions. However, under reducing conditions, the catalytic rate after the anodic polarization stabilized at an open circuit value higher than that observed before polarization, thus showing a light permanent EPOC behavior [51]. This might be due to a partially reduced state of the catalyst that was shown to be more active in pulsed experiments [52]. A partially reduced state of the catalyst should induce a higher density of electrons in the conduction band of the particles that would enable easier extraction of electrons from palladium species compared to the fully oxidized PdO . Indeed, this is consistent with the shift in the binding energy of the electrons in the used sample observed in

the XPS spectra in Fig. 4a demonstrated to be caused by a metallic palladium core both by depth-profiling XPS and XRD experiments.

Figs. 8–10 show the dependence of the current on the catalyst overpotential, η , at three different temperatures, under reducing, stoichiometric and oxidizing conditions, respectively. The overpotential is defined as (Eq. (4)):

$$\eta = U_{\text{WR}} - U_{\text{WR}}^0 - IR \quad (4)$$

where U_{WR}^0 and U_{WR} is the potential between the working and reference electrodes under open circuit and polarization conditions, respectively; I is the applied current and R is the resistance of the sample.

As observed in Figs. 8–10 at 350 °C, independent on the gas composition, the CO₂ formation rate increases under positive polarization, while negative polarization results in a decrease of the catalytic activity, indicating again electrophobic behavior, as observed during the galvanostatic transients.

It is also worth noting that the negative polarization does not always lead to a decrease in reaction rate. As shown in Fig. 8, at temperatures higher than 400 °C for operation under excess of methane, the application of negative potentials leads to an increase in the CO₂ formation rate. According to the literature, this behavior indicates an inverted volcano nature of the reaction [25]. Similar results were obtained by Frantzis et al. [32] while working above 400 °C under fuel-rich conditions. The observed inverted volcano behavior can be explained since at high temperatures under reducing conditions the methane oxidation is controlled by a competitive adsorption of methane and oxygen leading to comparable low coverage of both species on the catalyst surface. Thus, both acceptor reactant species (O_{ads}) and donor reactant species (CH₄) are weakly adsorbed on the catalytic surface, and both anodic and cathodic polarizations lead to an increased reaction rate [25]. As already described in the literature [48], dissociative adsorption of CH₄ occurs more effectively on metallic Pd than on bulk PdO, and, once formed, the fragments of the dissociative adsorption of CH₄ spill over onto the surface and become rapidly reduced.

4. Conclusions

The effect of electrochemical promotion of catalysis (NEMCA effect or EPOC) has been studied for methane oxidation on Pd catalytic films interfaced with highly porous YSZ, at temperatures ranging from 350 to 430 °C, under reducing, stoichiometric and oxidizing conditions. The present study has revealed for the first time that the wet impregnation of palladium on highly porous YSZ allows obtaining a much more active catalyst than that typically prepared on dense YSZ, i.e. the catalytic rate being, under similar working conditions (metal loading, temperature and gas composition), one order of magnitude higher in the case of impregnated sample on porous YSZ than the one observed on dense YSZ. This catalytic performance improvement is related to the much higher dispersion of the catalyst (up to 450%) obtained for catalysts supported on porous electrolytes.

Despite its unusually high intrinsic activity and considerable in-plane resistance, the catalyst dispersed on the porous interlayered support can still be electrochemically promoted by positive polarizations, providing a reaction rate enhancement up to 50%. The results obtained under positive polarization are consistent with the kinetics of methane oxidation on Pd based catalyst.

Under fuel rich conditions, a permanent NEMCA is noticed, which was found to be due to the presence of a palladium metallic core covered by surface oxide; the metal core, likely induces a higher density of electrons in the conduction band of the particles, which enables easier extraction of electrons from surface palladium species compared to the fully oxidized PdO. The presence in the

used sample of the palladium metallic core covered by a surface oxide was confirmed by the depth-profiling XPS analysis.

Even though the reaction shows electrophobic behavior, similar to the dense YSZ sample, at temperatures higher than 400 °C under fuel rich conditions, the application of negative potentials also leads to an increase in the CO₂ formation rate. This behavior was attributed to the competitive adsorption of methane and oxygen under these reaction conditions.

Acknowledgments

Financial support by Romanian Government [Project POS-DRU/88/1.5/S/56661] and Science and Innovation Ministry of Spain [Project CTQ2007-62512/PPQ and MAT2010-19837-C06-04] are gratefully acknowledged. The authors would like to thank Prof. Costas Vayenas for fruitful discussions of these results.

Appendix A. Supplementary data

Supplementary data associated with this article can be found, in the online version, at <http://dx.doi.org/10.1016/j.apcatb.2012.11.011>.

References

- [1] Y.H. Chin, D.E. Resasco, *Catalysis* 14 (1999) 1–39.
- [2] J.H. Lee, D.L. Trimm, *Fuel Processing Technology* 42 (1995) 339–359.
- [3] P. Forzatti, *Catalysis Today* 83 (2003) 3–18.
- [4] P. Forzatti, G. Groppi, *Catalysis Today* 54 (1999) 165–180.
- [5] J.K. Lampert, M.S. Kazi, R.J. Farrauto, *Applied Catalysis B: Environmental* 14 (1997) 211–223.
- [6] P. Gélin, L. Urfeis, M. Primet, E. Tena, *Catalysis Today* 83 (2003) 45–57.
- [7] T.V. Choudhary, S. Banerjee, V.R. Choudhary, *Applied Catalysis A: General* 234 (2002) 1–23.
- [8] P. Gélin, M. Primet, *Applied Catalysis B: Environmental* 39 (2002) 1–37.
- [9] D. Ciuparu, M.R. Lyubovsky, E. Altman, L.D. Pfefferle, A. Datye, *Catalysis Reviews* 44 (2002) 593–649.
- [10] Z. Li, G.B. Hoflund, *Journal of Natural Gas Chemistry* 12 (2003) 153–160.
- [11] N.V. Vegten, M. Maciejewski, F. Krumeich, A. Baiker, *Applied Catalysis B: Environmental* 93 (2009) 38–49.
- [12] S. Colussi, A. Trovarelli, E. Vesselli, A. Baraldi, G. Comelli, G. Groppi, J. Llorca, *Applied Catalysis A: General* 390 (2010) 1–10.
- [13] C.A. Müller, M. Maciejewski, R.A. Koepel, A. Baiker, *Catalysis Today* 47 (1999) 245–252.
- [14] D. Ciuparu, L. Pfefferle, *Catalysis Today* 77 (2002) 167–179.
- [15] M. Lyubovsky, L. Pfefferle, *Applied Catalysis A: General* 173 (1998) 107–119.
- [16] D. Ciuparu, L. Pfefferle, *Applied Catalysis A: General* 209 (1–2) (2001) 415–428.
- [17] T.R. Baldwin, R. Burch, *Applied Catalysis* 66 (1990) 337–358.
- [18] C.F. Cullis, B.M. Willat, *Journal of Catalysis* 83 (1983) 267–285.
- [19] F.H. Ribeiro, M. Chow, R.A. Dalla Betta, *Journal of Catalysis* 146 (1994) 537–544.
- [20] K. Sekizawa, H. Widjaja, S. Maeda, Y. Ozawa, K. Eguchia, *Catalysis Today* 59 (2000) 69–74.
- [21] L.S. Escandón, S.r. Ordóñez, A. Vega, F.V. Díez, *Chemosphere* 58 (2005) 9–17.
- [22] N.M. Rodriguez, S.G. Oh, R.A. DallaBetta, R.T.K. Baker, *Journal of Catalysis* 157 (2) (1995) 676–686.
- [23] M. Stoukides, C.G. Vayenas, *Journal of Catalysis* 70 (1981) 137–146.
- [24] C.G. Vayenas, S. Bebelis, S. Ladas, *Nature* 343 (1990) 625–627.
- [25] C.G. Vayenas, S. Bebelis, C. Pliangos, S. Brosda, D. Tsipakidis, *Electrochemical Activation of Catalysis: Promotion, Electrochemical Promotion and Metal-Support Interactions*, Kluwer Academic/Plenum Publishers, New York, 2001.
- [26] G.L. Haller, *Journal of Catalysis* 216 (2003) 12–22.
- [27] J. Nicole, D. Tsipakidis, C. Pliangos, X.E. Verykios, Ch. Comninellis, C.G. Vayenas, *Journal of Catalysis* 204 (2001) 23–34.
- [28] A. Nakos, S. Sountzie, A. Katsaounis, *Applied Catalysis B: Environmental* 101 (2010) 31–37.
- [29] E.A. Baranova, G. Fóti, Ch. Comninellis, *Electrochemistry Communications* 6 (2004) 389–394.
- [30] P. Tsikararas, C.G. Vayenas, *Journal of Catalysis* 140 (1993) 53–70.
- [31] A. Giannikos, A.D. Frantzis, C. Pliangos, S. Bebelis, C.G. Vayenas, *Ionics* 4 (1998) 53–60.
- [32] A.D. Frantzis, S. Bebelis, C.G. Vayenas, *Solid State Ionics* 136/137 (2000) 863–872.
- [33] V. Roche, R. Karoum, A. Billard, R. Revel, P. Vernoux, *Journal of Applied Electrochemistry* 38 (2008) 1111–1119.
- [34] C. Jimenez-Borja, S. Brosda, M. Makri, F. Sapountzi, F. Dorado, J.L. Valverde, C.G. Vayenas, *Solid State Ionics* 225 (2012) 376–381.
- [35] M. Marwood, C.G. Vayenas, *Journal of Catalysis* 178 (1998) 429–440.

[36] I. Constantinou, I. Bolzonella, C. Pliangos, Ch. Comninellis, C.G. Vayenas, *Catalysis Letters* 100 (2005) 125–133.

[37] F. Dorado, A. de Lucas-Consuegra, C. Jiménez, J.L. Valverde, *Applied Catalysis A: General* 321 (2007) 86–92.

[38] C. Jiménez-Borja, F. Dorado, A. de Lucas-Consuegra, J.M. García-Vargas, J.L. Valverde, *Catalysis Today* 146 (2009) 326–329.

[39] C. Jimenez-Borja, S. Brosda, F. Matei, M. Makri, B. Delgado, F. Sapountzi, D. Ciuparu, F. Dorado, J.L. Valverde, C.G. Vayenas, *Applied Catalysis B: Environmental* 128 (2012) 48–54.

[40] E.I. Papaioannou, S. Souentie, F.M. Sapountzi, A. Hammad, D. Labou, S. Brosda, C.G. Vayenas, *Journal of Applied Electrochemistry* 40 (2010) 1859–1865.

[41] V. Jiménez, C. Jiménez-Borja, P. Sánchez, A. Romero, E.I. Papaioannou, D. Theleritis, S. Souentie, S. Brosda, J.L. Valverde, *Applied Catalysis B: Environmental* 107 (2011) 210–220.

[42] A. De Lucas-Consuegra, A. Caravaca, P.J. Martínez, J.L. Endrino, F. Dorado, J.L. Valverde, *Journal of Catalysis* 274 (2010) 251–258.

[43] S. Ladas, S. Bebelis, C.G. Vayenas, *Surface Science* 251 (1991) 1062–1068.

[44] J.A. Hinojosa Jr., J.F. Weaver, *Surface Science* 605 (2011) 1797–1806.

[45] F. Matei, D. Ciuparu, C. Jiménez-Borja, F. Dorado, J.L. Valverde, S. Brosda, *Applied Catalysis B: Environmental* 127 (2012) 18–27.

[46] V.S. Pamachandran (Ed.), *Handbook of Analytical Techniques in Concrete Science and Technology*, William Andrew Publishing, Noyes Publications, 2001.

[47] R. Jenkins, R.L. Snyder (Eds.), *Introduction to X Ray Powder Diffractometry*, Wiley, New York, 1996.

[48] S. Su, J. Carstens, A. Bell, *Journal of Catalysis* 176 (1998) 125–135.

[49] NIST on-Line XPS Database in National Institute of Standards and Technology.

[50] M. Peuckert, *Journal of Physical Chemistry* 89 (1985) 2481–2486.

[51] C. Falgairette, A. Jaccoud, G. Fóti, Ch. Comninellis, *Journal of Applied Electrochemistry* 38 (2008) 1075–1082.

[52] D. Ciuparu, L. Pferfferle, *Applied Catalysis A: General* 218 (2001) 197–209.